


Visualization of multiple organ amyloid involvement in systemic amyloidosis using ^{11}C -PiB PET imaging

Naoki Ezawa¹ · Nagaaki Katoh¹  · Kazuhiro Oguchi² · Tsuneaki Yoshinaga¹ · Masahide Yazaki^{3,4} · Yoshiki Sekijima^{1,2,4}

Received: 8 May 2017 / Accepted: 21 August 2017 / Published online: 10 September 2017
© Springer-Verlag GmbH Germany 2017

Abstract

Purpose To investigate the utility of Pittsburgh compound B (PiB) positron emission tomography (PET) imaging for evaluating whole-body amyloid involvement in patients with systemic amyloidosis.

Methods Whole-body ^{11}C -PiB PET was performed in seven patients with systemic immunoglobulin light-chain (AL) amyloidosis, seven patients with hereditary transthyretin (ATTRm) amyloidosis, one asymptomatic *TTR* mutation carrier and three healthy controls. The correlations between clinical organ involvement, radiological ^{11}C -PiB uptake and histopathological findings were analysed for each organ.

Results Organ involvement on ^{11}C -PiB PET imaging showed good correlations with the clinical findings for the heart and stomach. Abnormal tracer uptake was also observed in the spleen, lachrymal gland, submandibular gland, sublingual gland, lymph node, brain, scalp, extraocular muscles, nasal mucosa, pharynx, tongue and nuchal muscles, most of which were asymptomatic. Physiological tracer uptake was universally observed in the urinary tract (kidney, renal pelvis, ureter and bladder) and enterohepatic circulatory system (liver,

gallbladder, bile duct and small intestine) in all participants. Most of the patients and one healthy control subject showed asymptomatic tracer uptake in the lung and parotid gland. The peripheral nervous system did not show any tracer uptake even in patients with apparent peripheral neuropathy. Histological amyloid deposition was confirmed in biopsied myocardium and gastric mucosa where abnormal ^{11}C -PiB retention was observed.

Conclusions ^{11}C -PiB PET imaging can be used clinically in the systemic evaluation of amyloid distribution in patients with AL and ATTRm amyloidosis. Quantitative analysis of ^{11}C -PiB PET images may be useful in therapy evaluation and will reveal whether amyloid clearance is correlated with clinical response.

Keywords Amyloid · Pittsburgh compound B PET · Amyloid imaging · Light-chain amyloidosis · Hereditary transthyretin amyloidosis

Introduction

Systemic amyloidosis is a group of diseases associated with progressive deposition of circulating amyloid precursor protein in a number of vital organs, which eventually results in fatal multiple organ dysfunction unless properly treated. Appropriate diagnosis and treatment at the early stage are therefore critically important to improve prognosis. To develop an adequate treatment plan, it is essential to confirm amyloid deposition and to evaluate the extent of organ involvement. At present, histopathological examination of biopsied tissue specimens is performed to confirm amyloid deposition. However, this has a number of limitations, including relatively high invasiveness and the requirement for specific operator skills. In addition, tissue

✉ Nagaaki Katoh
nagaaki@shinshu-u.ac.jp

¹ Department of Medicine (Neurology and Rheumatology), Shinshu University School of Medicine, 3-1-1 Asahi, Matsumoto, Nagano 390-8621, Japan
² Jisenkai Brain Imaging Research Center, 2-5-1 Honjyo, Matsumoto, Japan
³ Department of Biomedical Laboratory Sciences, Shinshu University School of Health Sciences, 3-1-1 Asahi, Matsumoto, Japan
⁴ Institute for Biomedical Sciences, Shinshu University, 3-1-1 Asahi, Matsumoto, Japan

Table 1 Clinical background, organ involvement, and ¹¹C-PiB tracer uptake in the enrolled subjects

No.	Diagnosis	Age	Sex	Treatment history	Organ involvement and PiB tracer uptake																			
					Glandular tissues						CNS			PNS			Soft tissues							
					Ht	St	Sp	LG	PG	SmG	SIG	TG	LN	Brain	SmN	AN	Sc	EM	Na	Ph	Tg	NM		
1	Systemic AL amyloidosis	56	M	Chemotherapy	Organ involvement	+	+						(+)			+	+					+		
					Tracer uptake	+++	+	++	+	+				+++								+		
2	Systemic AL amyloidosis	71	M	None	Organ involvement	+							(+)										+	++
					Tracer uptake	++			+	+														
3	Systemic AL amyloidosis	82	F	None	Organ involvement	+							(+)									+	(+)	
					Tracer uptake	+		+								++								
4	Systemic AL amyloidosis	52	F	None	Organ involvement	+	+				(+)		(+)											
					Tracer uptake	+	+	+			+	+									+			
5	Systemic AL amyloidosis	69	F	None	Organ involvement	+																		
					Tracer uptake	++	+		+															
6	Systemic AL amyloidosis	59	M	None	Organ involvement	+							(+)											
					Tracer uptake	+++		++	+			+												
7	Systemic AL amyloidosis	57	F	None	Organ involvement																			
					Tracer uptake																			
8	Hereditary ATTR amyloidosis (V30M)	43	F	LDLT	Organ involvement	+	+						(+)			+	+							
					Tracer uptake	++	+		+															
9	Hereditary ATTR amyloidosis (V30M)	45	M	LDLT, Tafamidis	Organ involvement	+	+						(+)			+	+							
					Tracer uptake	++	+		+	++	++			++		+				+	+	++	+	
10	Hereditary ATTR amyloidosis (G47R)	23	F	Tafamidis	Organ involvement	+	+			(+)			(+)			+	+							
					Tracer uptake	+	++	+	+	+		+												
11	Hereditary ATTR amyloidosis (V30M)	43	M	LDLT	Organ involvement	+										+	+							
					Tracer uptake	+++	+		+	+++	+++		+++								+	+	++	+
12	Hereditary ATTR amyloidosis (V30M)	43	M	BDLT	Organ involvement	+										+	+							
					Tracer uptake	+++	+		++	+++	+++	++	+++								+	+	++	+
13	Hereditary ATTR amyloidosis (V30M)	55	M	BDLT, PM, Tafamidis	Organ involvement	+	+									+	+							
					Tracer uptake	+++	+		++	+		+			+									
14	Hereditary ATTR amyloidosis (T60A)	58	M	None	Organ involvement	+	+										+							
					Tracer uptake	+	+		+															
15	Asymptomatic <i>TTR</i> mutation carrier (D18G)	28	F	None	Organ involvement																			
					Tracer uptake																			
16	Healthy control	39	M	None	Organ involvement																			
					Tracer uptake																			
17	Healthy control	38	M	None	Organ involvement																			
					Tracer uptake						+													
18	Healthy control	50	M	None	Organ involvement																			
					Tracer uptake																			

PiB Pittsburgh compound B, *AL amyloidosis* light-chain amyloidosis, *ATTR amyloidosis* transthyretin amyloidosis, *Ht* heart, *St* stomach, *Sp* spleen, *LG* lachrymal gland, *PG* parotid gland, *SmG* submandibular gland, *SIG* sublingual gland, *TG* thyroid gland, *LN* lymph node, *CNS* central nervous system, *PNS* peripheral nervous system, *SmN* sensorymotor neuropathy, *AN* autonomic neuropathy, *Sc* scalp, *EM* extraocular muscles, *Na* nasal mucosa, *Ph* pharynx, *Tg* tongue, *NM* nuchal muscles, *LDLT* living-donor partial liver transplantation, *BDLT* brain-dead donor liver transplantation, *PM* pacemaker, Tracer uptake grading: +: mild; ++: moderate; +++: intense, Gray boxes: organ involvements not determined by international consensus criteria [7]; (+): organ-related symptoms without consensus involvement criteria

biopsy can be used to evaluate amyloid deposition only in a limited area of a single organ. Therefore, whole-body amyloid imaging is becoming a novel, useful, and less invasive method for evaluating systemic amyloidosis.

¹¹C-Labelled Pittsburgh compound B (¹¹C-PiB; 2-[4'-methylaminophenyl]-6-hydroxybenzothiazole) positron emission tomography (PET) is an established amyloid imaging technique used in the evaluation of localized Aβ amyloid deposition in the brain of patients with Alzheimer's disease [1] and Aβ-type cerebral amyloid angiopathy [2]. PiB is a derivative of the amyloid-binding dye, thioflavin-T [3], and it can therefore theoretically combine with various amyloid proteins. Recent studies have indicated that PiB is able to detect other types of amyloidosis [4–6]. In the study reported here we investigated the feasibility of using ¹¹C-PiB PET in the evaluation of whole-body amyloid deposition in two major types of systemic amyloidosis, i.e. systemic immunoglobulin light-chain (AL) and hereditary transthyretin (ATTRm) amyloidosis.

Materials and methods

Participants

The clinical information of the participants is summarized in Table 1. From June 2015 to December 2016, seven patients with histologically proven systemic AL amyloidosis (mean ± SD age 63.7 ± 10.6 years, range 52–82 years), seven patients with histologically and genetically proven ATTRm amyloidosis (age 44.3 ± 11.3 years, range 23–58 years), one asymptomatic *TTR* gene mutation carrier (age 28 years) and three healthy control volunteers (age 42.3 ± 6.7 years, range 38–50 years) were enrolled in this study. All patients were diagnosed and examined at Shinshu University Hospital. All of the AL amyloidosis patients were newly diagnosed untreated patients except one (subject 1, Table 1) who had received chemotherapy but relapsed before achieving any clinical organ response. The *TTR* genotypes of the ATTRm amyloidosis patients were as follows: V30M (p.V50M) heterozygous (five patients), G47R (p.G67R) heterozygous (one

patient), and T60A (p.T80A) heterozygous (one patient). All ATTRm patients except one (subject 14) received anti-amyloid therapies, liver transplantation and/or tafamidis (Table 1). The *TTR* genotype of the asymptomatic mutation carrier (subject 15, Table 1) was D18G (p.D38G).

Clinical evaluation

Clinical organ involvement due to systemic amyloid deposition was evaluated in all participants at the time of the scan. The international consensus guidelines from the 10th International Symposium on Amyloid and Amyloidosis [7] were used to determine organ involvement of the heart, kidney, liver, gastrointestinal tract, lung, sensorimotor and autonomic nervous system, tongue and lymph nodes (Table 2). Reduced gastric motility was demonstrated gastroendoscopically by confirming residual gastric contents ingested on the day before gastroendoscopy. These criteria were originally designed for evaluating AL amyloidosis. However, we used these criteria for evaluating both AL and ATTRm amyloidosis in this study as no established evaluation method was available for ATTRm amyloidosis. With regard to other organs without consensus involvement criteria, organ-related symptoms were simply described, but possible correlations between symptoms and amyloid involvement are not discussed.

¹¹C-PiB PET imaging

All imaging was performed with a PET/CT scanner (Discovery PET/CT 600; GE Healthcare, Milwaukee, WI). A whole-body low-dose CT scan from the vertex to the pelvis was performed 30 min after administration of 500–636 MBq of ¹¹C-PiB. After the CT scan, emission scans with seven bed positions were followed by a scan at 2 min per bed position in 3D mode. The images were reviewed by trained amyloidologists and a radiologist from among the authors (N.E, N.K, K.O and Y.S). Both maximum intensity projection images (Fig. 1) and transaxial images (Fig. 2) were visually examined in the conventional manner to evaluate tracer uptake in the body. For brain evaluation, standardized uptake value ratio (SUVR) images (Fig. 2Aa, Ba, Ca) were generated by normalizing ¹¹C-PiB uptake relative to pontine uptake [2], because ¹¹C-PiB uptake in the brain was weaker than in the other involved organs (Figs. 1 and 2) and abnormal ¹¹C-PiB retention was observed in the cerebellum but not in the pons in ATTRm amyloidosis patients [6]. In this study, only leptomeningeal brain uptake [6], and not uptake characteristic of Alzheimer's disease, was taken as significantly positive brain uptake because we intended to evaluate amyloid deposition derived from systemic amyloidosis and not that derived from localized A β amyloidosis. Tracer uptake in the scalp was determined as significantly positive only when the uptake was stronger than in the brain white matter on SUVR images (Fig.

Table 2 Organ involvement criteria in this study determined according to international consensus guidelines [7]

Organ	Criterion for organ involvement
Heart	Mean left ventricular wall thickness > 12 mm, no other cardiac cause
Kidney	24-h urine protein >0.5 g/day, predominantly albumin
Liver	Total liver span >15 cm or alkaline phosphatase >1.5 times institutional upper limit of normal
Gastrointestinal tract	Direct biopsy verification with symptoms
Lung	Direct biopsy verification with symptoms, Interstitial radiographic pattern
Nerve	Peripheral: clinical; symmetrical lower extremity sensorimotor peripheral neuropathy Autonomic: gastric-emptying disorder, pseudo-obstruction, voiding dysfunction not related to direct organ infiltration
Tongue	Tongue enlargement, clinical
Lymph node	Lymphadenopathy

2Ca). Abnormal tracer uptake was graded visually as mild (+), moderate (++) or intense (+++; Table 1).

Histopathological analysis

The correlations between histopathological findings of biopsied specimens and ¹¹C-PiB PET findings were investigated retrospectively to validate the feasibility of ¹¹C-PiB PET. Histopathological analysis, including Congo red staining and immunohistochemical staining, was performed as described previously [8].

Protocol approval and patient consent

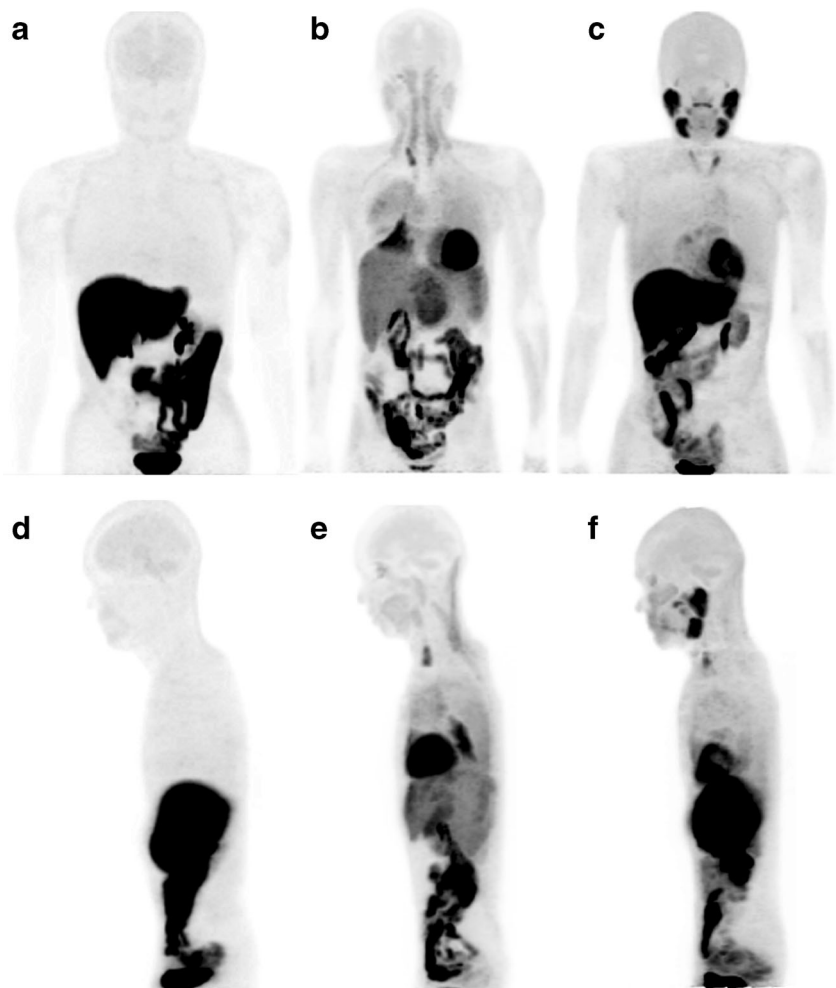
All procedures in studies involving human participants were performed in accordance with the ethical standards of the institutional and/or national research committee and with the principles of the 1964 Declaration of Helsinki and its later amendments or comparable ethical standards. The study protocol was approved by the Ethics Committee of Shinshu University School of Medicine, and written informed consent was obtained from each participant.

Results

Correlations between clinical manifestations and ¹¹C-PiB PET images

The clinical background of the participants, organ involvement, and ¹¹C-PiB tracer uptake in each organ are summarized in Table 1. Universal tracer uptake was observed in the urinary

Fig. 1 Representative whole-body maximum intensity projection ^{11}C -PiB PET images: **a** – **c** anterior views; **d** – **f** lateral views; **a, d** healthy control subject (subject 16, Table 1); **b, e** AL amyloidosis patient (subject 1, Table 1); **c, f** ATTRm amyloidosis patient (subject 12, Table 1). The urinary tract and enterohepatic circulatory system are positively delineated in all subjects due to the physiological clearance pathway of ^{11}C -PiB. Abnormal tracer uptake in the heart, spleen, extraocular muscles, parotid gland, tongue, nuchal muscles, submandibular gland and thyroid gland is apparent in the AL patient (**b, e**). Increased density due to collapse of the lower right lung is also apparent (**b, e**). Abnormal tracer uptake in the heart, scalp, lachrymal gland, parotid gland, nasal mucosa, pharynx, tongue, submandibular gland, sublingual gland, thyroid gland and brain is apparent in the ATTRm patient (**c, e**)



tract (kidney, renal pelvis, ureter and bladder) and enterohepatic circulatory system (liver, gallbladder, bile duct and small intestine) in all participants, including healthy controls (Figs. 1 and 2) due to physiological clearance of ^{11}C -PiB through the renal and hepatobiliary systems [9]. In addition, most of the patients with systemic amyloidosis and one healthy control subject showed increased ^{11}C -PiB retention in the lung (Fig. 2Ah, Bh, Ch). This was probably due to reduced pulmonary blood flow and a partial volume effect induced by a collapsed lung. For these reasons, we excluded the urinary tract, enterohepatic circulatory system and lung from the evaluations.

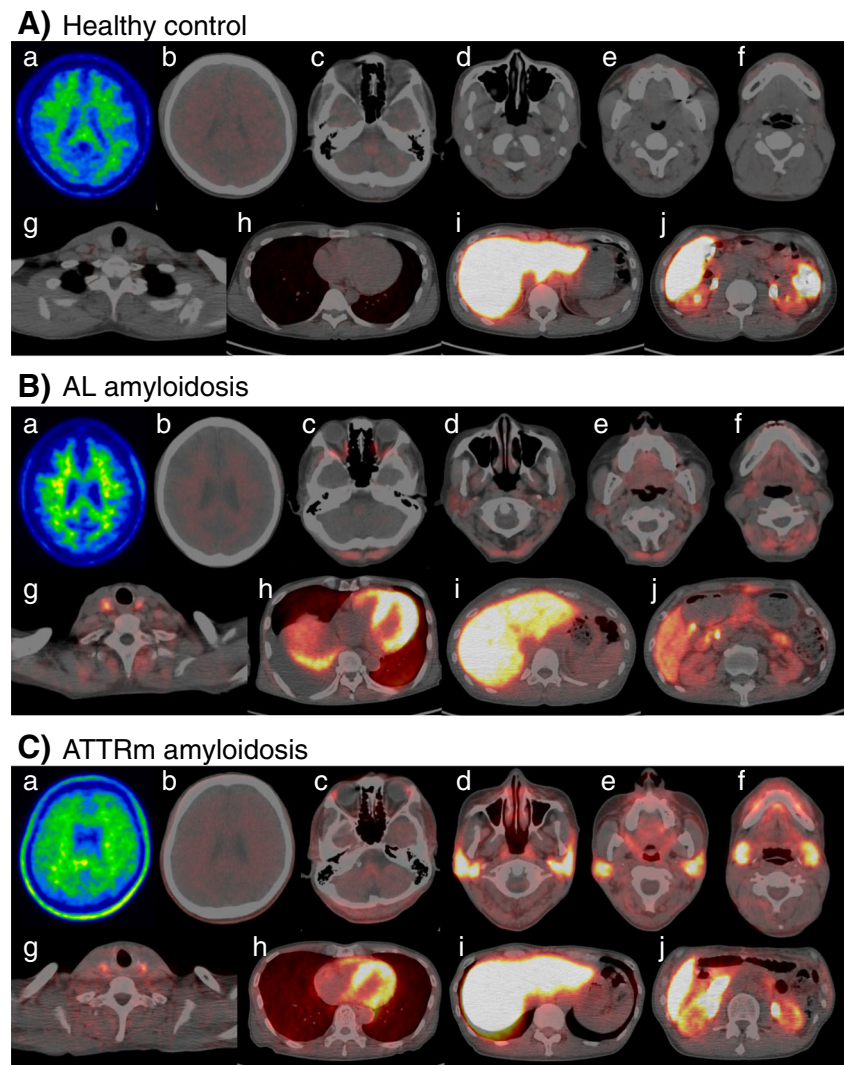
Common findings for both AL and ATTRm amyloidosis

Among the organs evaluated, good correlations between clinical and radiological organ involvement were observed in the heart (Fig. 2Bh, Ch) and stomach (Fig. 2Bi, Ci) in both AL and ATTRm amyloidosis. As shown in Table 1, 11 of 12 patients with clinical cardiac involvement (mean left ventricular wall thickness >12 mm) showed positive tracer uptake in the heart. The only exception was a 23-year-old

female ATTRm patient with G47R mutation (subject 10, Table 1) who did not show increased ^{11}C -PiB retention, although she presented with mild cardiac wall thickening (mean left ventricular wall thickness 14.5 mm), compatible with amyloid cardiomyopathy. Similarly, all eight patients with clinical gastric involvement (decreased gastric motility) showed positive gastric ^{11}C -PiB uptake. In addition, two patients (one AL and one ATTRm) showed increased ^{11}C -PiB retention in the gastric wall, although they did not have clinical gastric involvement. Radiological involvement was more sensitive than clinical organ involvement in the tongue, as 13 patients (six AL, seven ATTRm) showed increased ^{11}C -PiB retention in the tongue (Figs. 1e, f, 2Be, Ce) and two (both AL) had obvious macroglossia (Table 1).

It is likely that ^{11}C -PiB PET is able to detect subclinical amyloid deposition in glandular tissues. The salivary glands (parotid gland, submandibular gland and sublingual gland) were the most prominent organs positive for ^{11}C -PiB, and increased retention was observed in four AL and six ATTRm patients. Among these patients, the submandibular gland was palpable in one AL patient. The

Fig. 2 Representative transaxial PET images and fused PET/CT images. **A** Healthy control (subject 16, Table 1); **B** AL amyloidosis patients (**Ba–h, j** patient 1; **Bi** patient 4; Table 1). **C** ATTRm amyloidosis patients (**Ca, b** patient 9; **Cc–j** patient 12; Table 1). Increased ^{11}C -PiB retention is apparent in the brain (**Ca**), scalp (**Ca, b**), lachrymal gland (**Cc**), extraocular muscles (**Bc**), nuchal muscles (**Bc–g**), parotid gland (**Ad–e, Bd–e, Cd–e**), nasal mucosa (**Cd**), pharynx (**Cd–f**), tongue (**Be** and **Ce**), submandibular gland (**Bf, Cf**), sublingual gland (**Cf**), thyroid gland (**Bg, Cg**), heart (**Bh, Ch**), lung (**Ah, Bh, Ch**), liver (**Ai–j, Bi–j, Ci–j**), gastric wall, spleen (**Bi, Ci**), small intestine, and kidneys (**Aj, Bj, Cj**)



amount of ^{11}C -PiB accumulation in the salivary glands in ATTRm patients (Fig. 2Cd–f) was greater than in AL patients (Fig. 2Bd–f). One healthy control subject showed ^{11}C -PiB retention in the parotid gland, but the level was much lower than in patients with systemic amyloidosis. Eight patients (three AL, five ATTRm) showed increased ^{11}C -PiB retention in the thyroid (Fig. 2Bg, Cg), and five of these patients (three AL, two ATTRm) had subclinical hypothyroidism (Table 1). Six patients (four AL, two ATTRm; Fig. 2Bi) showed positive ^{11}C -PiB accumulation in the spleen, but none of the patients showed clinical symptoms regarding this organ.

In contrast to other organs, amyloid deposition in the peripheral nervous system was difficult to detect by ^{11}C -PiB PET. In fact, no patients showed increased ^{11}C -PiB retention in the peripheral nervous system (i.e. nerve root, plexus and peripheral nerves), although six ATTRm patients and one AL patient showed clinically obvious sensorimotor and autonomic polyneuropathy.

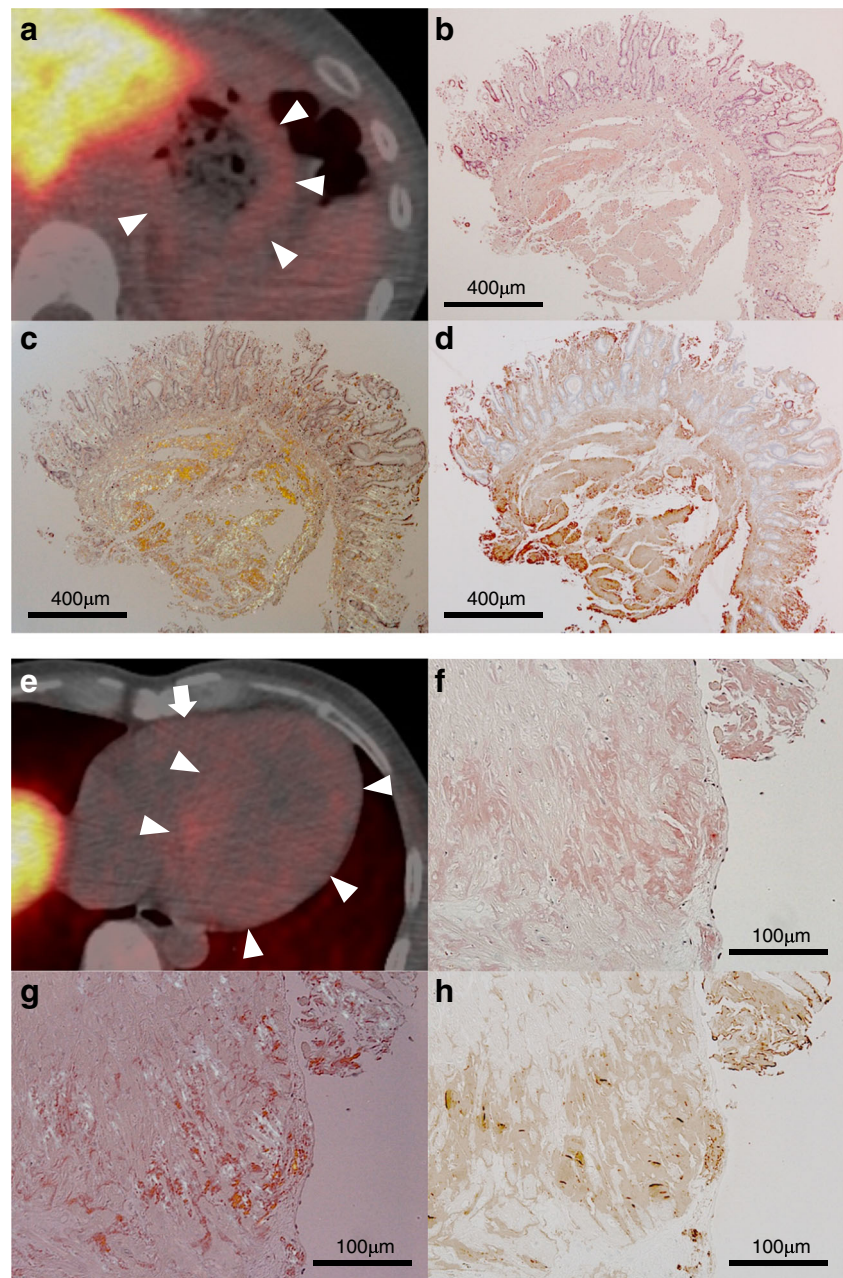
Specific findings for AL amyloidosis

Characteristic abnormal ^{11}C -PiB accumulation in the nuchal muscles (Figs. 1b, e, 2Bc–g) was observed only in five patients with AL amyloidosis, and one of these patients showed a dropped head due to weakness of the nuchal muscles. Lymph nodes (one patient) and extraocular muscles (two patients; Figs. 1e, 2Bc) were the other organs in which positive ^{11}C -PiB uptake was observed only in patients with AL amyloidosis, and none of these patients showed clinical symptoms regarding these organs.

Specific findings for ATTRm amyloidosis

Abnormal ^{11}C -PiB retention was observed only in ATTRm amyloidosis patients in the lachrymal gland (five patients; Fig. 2Cc), brain (two patients; Fig. 2Ca), scalp (three patients; Fig. 2Ca), nasal mucosa (three patients; Figs. 1f, 2Cd), and pharynx (four patients; Fig. 2Cd–f; Table 1).

Fig. 3 Correlations between ^{11}C -PiB PET images and histopathological findings. **a – d** Gastric images in an AL amyloidosis patient (patient 4, Table 1). Transaxial fused PET/CT image of the stomach (**a**) shows mild ^{11}C -PiB tracer uptake in the gastric wall (arrowheads). Congo red staining of biopsied gastric mucosa specimen shows considerable amyloid deposition in muscularis mucosae, submucosal connective tissue and lamina propria (**b, c** polarized view), and all of these deposits are specifically immunolabelled with anti- $\text{A}\lambda$ antibody (**d**; scale bars **b – d** 400 μm). **e – h** Cardiac images in an ATTRm amyloidosis patient (patient 14, Table 1). Transaxial fused PET/CT image of the heart (**e**) shows mild ^{11}C -PiB tracer uptake in the left ventricular wall and intraventricular septum (arrowheads) and in the anterior wall of the right ventricle (arrow). Congo red staining of biopsied endomyocardial specimen shows moderate amyloid deposition in interstitial tissue around cardiomyocytes (**f, g** polarized view). All of these deposits are specifically immunolabelled with anti-TTR antibody (**h** scale bars **f – h** 100 μm)



None of the patients showed clinical symptoms regarding these organs, except one patient with positive lachrymal gland uptake who showed dry eye.

Correlation between ^{11}C -PiB PET images and histopathological findings

To validate the feasibility of whole-body ^{11}C -PiB PET in the detection of amyloid deposition, we investigated the correlation between ^{11}C -PiB PET images and histopathological findings in biopsied tissues. In this study, gastric mucosal biopsy specimens were available in ten patients (three AL, seven ATTRm)

and an endomyocardial biopsy specimen was available in one ATTRm patient. Considerable amyloid deposition was observed in muscularis mucosae and submucosal connective tissue in all gastric mucosal biopsy specimens, and abnormal ^{11}C -PiB retention in the gastric wall was observed in each patient (Fig. 3a – d). Endomyocardial biopsy was performed in a 58-year-old male ATTRm patient (patient 14, Table 1) with a 2-year history of cardiac dysfunction. Histopathological examination demonstrated moderate ATTR amyloid deposition in the cardiac interstitium and ^{11}C -PiB PET showed abnormal tracer retention in the cardiac wall, compatible with the histopathological findings (Fig. 3e – h).

Table 3 Amyloid imaging techniques for systemic amyloidosis

Tracer	Type of amyloidosis	Advantages	Limitations	Reference
¹²³ I-SAP	AL and AA	Amyloid detectable in the spleen, kidneys, adrenals, bone marrow, carpal region, skin, and tongue	Heart undetectable. Positive liver scintigraphy observed even among patients whose liver function (including ALP) is totally normal	[10]
	ATTRm	Amyloid detectable in the spleen, kidneys, and adrenals	Heart, GI tract, and nerves undetectable. Liver scintigraphy positive in all patients whose hepatic amyloid was histologically confirmed to be absent	[11]
	Aβ2M	Amyloid detectable in the affected joints (wrists and knees) and spleen	Low sensitivity for detecting shoulder and hip joint arthropathy	[12]
	AApo-AI	Amyloid detectable in the spleen, kidneys, and liver	Amyloid deposition undetectable in the skin, vocal cords, heart, nerves, and testes	[13]
^{99m} Tc-DPD	AL	Amyloid detectable in the skeletal muscle	About half of patients with cardiac involvement did not show positive scintigraphy. The other visceral organs showed negative uptake	[14]
	ATTRm	Amyloid detectable in the heart, joints, lower GI tract, thoracic and abdominal wall	No significant liver or spleen uptake in patients. Physiological positive uptake in the urinary tract (kidney, ureter, and bladder) in patients and controls	[15]
	AApo-AI	Amyloid detectable in the heart	Data unknown for hepatic, renal, and neuropathic involvement	[16]
^{99m} Tc-PYP	AL	Amyloid detectable in the spleen, limbs, tongue, and thyroid	No significant correlation between cardiac amyloidosis and cardiac uptake. Limited relationship between organ involvement and tracer uptake in the liver, GI tract, and kidneys	[17, 18]
	ATTRm and ATTRwt	Cardiac involvement is sensitively detectable	Ability to detect organ involvement other than the heart is undetermined	[19, 20]
^{99m} Tc-MDP	AL and AA	Amyloid detectable in the limbs, tongue, and thyroid	No significant correlation between cardiac amyloidosis and cardiac uptake. Limited relationship between organ involvement and tracer uptake in the liver, GI tract, and kidneys	[18]
	AL and ATTR	Amyloid detectable in the heart in both AL and ATTR amyloidosis	Data unknown for other organs	[21, 22]
¹⁸ F-Florbetapir	AL	Amyloid detectable in the peripheral nerve and possibly in the muscles	Number of investigated patients limited to one (case report)	[23]
	AL	Amyloid detectable in the heart and larynx	Number of investigated patients limited to one (case report)	[24]
	ALECT2	Positive uptake observed in the lungs, spleen, adrenal glands, kidneys, and bone marrow	Number of investigated patients limited to one (case report)	[25]
	AL	Positive uptake observed in the heart, spleen, thyroid, salivary gland, and kidney	Number of investigated patients limited to one (case report)	[26]
^{99m} Tc-Aprotinin	AL (and ATTRm)	Amyloid detectable in the heart, pleura, lung, thyroid, pericardium, sternum, tongue, salivary glands, lymph node, oropharynx, larynx, intestines, and joints	Number of investigated patients with ATTRm very limited. Organs under the diaphragm (such as kidney, liver, spleen) not evaluable due to the high scattering from the kidneys. Central or peripheral nervous system involvement undetectable	[27, 28]
¹¹ C-PiB	AL and ATTRm	Good correlation between clinical and radiological involvement in the heart and stomach. Positive uptake in the tongue, lymph node, spleen, lachrymal gland, salivary glands, thyroid, brain, scalp, extraocular muscles, nasal mucosa, pharynx, and nuchal muscles	Physiological uptake in the lung, urinary tract, and enterohepatic circulation system. Peripheral nervous system involvement undetectable	This study

SAP serum amyloid P, DPD diphosphono-1,2-propanodicarboxylic acid, PYP pyrophosphate, MDP methylene diphosphonate, PiB Pittsburgh compound B, AL light-chain amyloidosis, AA serum amyloid A amyloidosis, ATTRm hereditary transthyretin amyloidosis, Aβ2M β2-microglobulin amyloidosis, AApo-AI apolipoprotein A I amyloidosis, ATTRwt systemic wild-type transthyretin amyloidosis, ALECT2 leucocyte cell-derived chemotaxin 2 amyloidosis, GI gastrointestinal

Discussion

Several previous studies have investigated the utility of whole-body molecular imaging to reveal systemic amyloid deposition using various tracers (Table 3) [10–28]. Scintigraphy with ^{123}I -labelled serum amyloid P component (^{123}I -SAP) is the most intensively investigated diagnostic test for whole-body amyloid imaging, and is able to detect amyloid deposition in several types of systemic amyloidosis, including AL, ATTRm, A β 2M and AApoAI amyloidosis [10–13]. However, ^{123}I -SAP scintigraphy is not sufficient to evaluate amyloid deposition in the heart [10, 11, 13], which is the most important organ for determining prognosis and therapeutic management in patients with systemic amyloidosis. In addition, the availability of ^{123}I -SAP is limited to certain specialized institutions [29].

Bone-seeking tracers, including $^{99\text{m}}\text{Tc}$ -3,3-diphosphono-1,2-propanodicarboxylic acid (DPD), $^{99\text{m}}\text{Tc}$ -pyrophosphate (PYP) and $^{99\text{m}}\text{Tc}$ -methylene diphosphonate (MDP), have also been reported to be useful for detecting systemic amyloidosis in ATTRm, wild-type ATTR (ATTRwt), AL and AApoAI amyloidosis [30]. Notably, bone-seeking tracers are very sensitive in the detection of cardiac ATTR amyloidosis [19, 20]. However, these tracers are unable to detect cardiac amyloid involvement in AL amyloidosis [14, 17, 18]. In addition, bone-seeking tracers are not useful for detecting amyloid deposition in most visceral organs other than the heart [14–18] (Table 3).

Recently, the potential of two ^{18}F -labelled tracers, ^{18}F -florbetapir [21–25] and ^{18}F -florbetaben [26], for whole-body amyloid imaging has been reported. Although ^{18}F -florbetapir PET was shown to be able to detect cardiac involvement in patients with AL and ATTRm amyloidosis [21], data concerning its ability to detect amyloid involvement of other organs are limited to case reports [23–25] (Table 3). Further experience in using this tracer for systemic amyloid evaluation in larger cohorts is needed. With regard to ^{18}F -florbetaben, there is only one case report of the positive uptake of the tracer in several organs in a patient with AL amyloidosis [26]. Further investigation of the correlation between ^{18}F -florbetaben uptake and histopathological findings in a group study setting is required. $^{99\text{m}}\text{Tc}$ -Aprotinin [27, 28] shows a similar uptake pattern to ^{11}C -PiB in AL amyloidosis patients (Table 3). However, its value for assessing ATTR amyloidosis is unclear due to the small number of patients investigated [27, 28], and this tracer is no longer used widely because of the withdrawal of bovine aprotinin from the market [22].

The greatest advantage of ^{11}C -PiB PET demonstrated in this study was that this widely available tracer can detect cardiac amyloid deposition very clearly in AL amyloidosis patients as well as in ATTRm amyloidosis patients. In addition, ^{11}C -PiB PET can reveal AL and ATTRm amyloid deposition in other organs, including the stomach, spleen, lymph nodes, brain, glandular tissues and soft tissues. In particular, it is

notable that there was a good correlation between clinical and radiological involvement in the stomach in both AL and ATTRm amyloidosis patients (Table 1). To our knowledge, there have been no reports of other tracers that can detect amyloid deposition in the gastric wall.

In this study, we confirmed the correlations between ^{11}C -PiB PET imaging findings and histopathological findings in the stomach and heart (Fig. 3). In addition, we recently showed that ^{11}C -PiB PET can detect leptomeningeal ATTR amyloid deposition with high sensitivity [6]. Other organs, including the spleen [31], lacrimal glands [32], salivary glands [33, 34], thyroid [35] and lymph nodes [36] have been reported to be histologically involved in patients with systemic amyloidosis. In this study, histological confirmation of amyloid deposition was not obtained from these organs, but they were positively delineated by ^{11}C -PiB PET only in patients with systemic amyloidosis, and not in the asymptomatic TTR mutation carrier or the healthy controls. Therefore, increased ^{11}C -PiB retention in these organs was considered to delineate amyloid deposition, and histological amyloid deposition in these organs may be more common than previously thought. However, detailed histology-based studies (biopsy and/or autopsy studies) are required to confirm the relationship between radiological tracer uptake intensity and histological amyloid burden in each organ.

This study identified several limitations of ^{11}C -PiB PET for clinical use in evaluating systemic amyloidosis. The first is its lack of ability to assess amyloid involvement in the urinary tract and enterohepatic circulatory system because of the physiological clearance pathway of PiB through the renal and hepatobiliary systems. This characteristic of ^{11}C -PiB PET could be a major limitation when evaluating patients with systemic AL amyloidosis, as both the kidney and liver are commonly involved in this disease [37, 38]. ^{11}C -PiB PET was also found to be unable to distinguish pathological lung uptake from physiological uptake, as not only amyloidosis patients but also one healthy control subject showed increased ^{11}C -PiB in the lung at similar intensities. Another limitation of ^{11}C -PiB PET is its inability to detect amyloid deposition in the peripheral nervous system, similar to previously reported tracers (Table 3).

In conclusion, ^{11}C -PiB PET imaging can be used clinically for systemic evaluation of amyloid distribution in AL and ATTRm amyloidosis patients. Quantitative analysis of ^{11}C -PiB PET may be useful in therapy evaluation and will reveal whether amyloid clearance is correlated with clinical response.

Funding This study was funded by a Grant-in-aid for Scientific Research (C) (23,591,237 to Y.S.) from the Japan Society for the Promotion of Science, a grant from the Amyloidosis Research Committee, the Ministry of Health, Labour and Welfare, Japan, and 2015 Global ASPIRE TTR-FAP Competitive Research Grant Award from Pfizer, Inc.

Compliance with ethical standards

Conflicts of interest None.

Ethical approval All procedures performed in studies involving human participants were in accordance with the ethical standards of the institutional and/or national research committee and with the principles of the 1964 Declaration of Helsinki and its later amendments or comparable ethical standards.

Informed consent Informed consent was obtained from all individual participants included in the study.

References

- Nordberg A, Carter SF, Rinne J, Drzezga A, Brooks DJ, Vandenberghe R, et al. A European multicentre PET study of fibrillar amyloid in Alzheimer's disease. *Eur J Nucl Med Mol Imaging*. 2013;40:104–14. <https://doi.org/10.1007/s00259-012-2237-2>.
- Johnson KA, Gregas M, Becker JA, Kinnecom C, Salat DH, Moran EK, et al. Imaging of amyloid burden and distribution in cerebral amyloid angiopathy. *Ann Neurol*. 2007;62:229–34. <https://doi.org/10.1002/ana.21164>.
- LeVine H III. Quantification of beta-sheet amyloid fibril structures with thioflavin T. *Methods Enzymol*. 1999;309:274–84.
- Antoni G, Lubberink M, Estrada S, Axelsson J, Carlson K, Lindsjö L, et al. In vivo visualization of amyloid deposits in the heart with ¹¹C-PIB and PET. *J Nucl Med*. 2013;54:213–20. <https://doi.org/10.2967/jnumed.111.102053>.
- Hellstrom-Lindahl E, Westermarck P, Antoni G, Estrada S. In vitro binding of [³H]PIB to human amyloid deposits of different types. *Amyloid*. 2014;21:21–7. <https://doi.org/10.3109/13506129.2013.860895>.
- Sekijima Y, Yazaki M, Oguchi K, Ezawa N, Yoshinaga T, Yamada M, et al. Cerebral amyloid angiopathy in posttransplant patients with hereditary ATTR amyloidosis. *Neurology*. 2016;87:773–81. <https://doi.org/10.1212/wnl.0000000000003001>.
- Gertz MA, Comenzo R, Falk RH, Fermand JP, Hazenberg BP, Hawkins PN, et al. Definition of organ involvement and treatment response in immunoglobulin light chain amyloidosis (AL): a consensus opinion from the 10th International Symposium on Amyloid and Amyloidosis, Tours, France, 18–22 April 2004, 18–22 April 2004. *Am J Hematol*. 2005;79:319–28. <https://doi.org/10.1002/ajh.20381>.
- Sekijima Y, Uchiyama S, Tojo K, Sano K, Shimizu Y, Imaeda T, et al. High prevalence of wild-type transthyretin deposition in patients with idiopathic carpal tunnel syndrome: a common cause of carpal tunnel syndrome in the elderly. *Hum Pathol*. 2011;42:1785–91. <https://doi.org/10.1016/j.humpath.2011.03.004>.
- Scheinin NM, Tolvanen TK, Wilson IA, Arponen EM, Nagren KA, Rinne JO. Biodistribution and radiation dosimetry of the amyloid imaging agent ¹¹C-PIB in humans. *J Nucl Med*. 2007;48:128–33.
- Hawkins PN, Lavender JP, Pepys MB. Evaluation of systemic amyloidosis by scintigraphy with ¹²³I-labeled serum amyloid P component. *N Engl J Med*. 1990;323:508–13. <https://doi.org/10.1056/nejm199008233230803>.
- Rydh A, Suhr O, Hietala SO, Ahlstrom KR, Pepys MB, Hawkins PN. Serum amyloid P component scintigraphy in familial amyloid polyneuropathy: regression of visceral amyloid following liver transplantation. *Eur J Nucl Med*. 1998;25:709–13.
- Nelson SR, Hawkins PN, Richardson S, Lavender JP, Sethi D, Gower PE, et al. Imaging of haemodialysis-associated amyloidosis with ¹²³I-serum amyloid P component. *Lancet*. 1991;338:335–9.
- Rowczenio D, Dogan A, Theis JD, Vrana JA, Lachmann HJ, Wechalekar AD, et al. Amyloidogenicity and clinical phenotype associated with five novel mutations in apolipoprotein A-I. *Am J Pathol*. 2011;179:1978–87. <https://doi.org/10.1016/j.ajpath.2011.06.024>.
- Hutt DF, Gilbertson J, Quigley AM, Wechalekar AD. (99m)Tc-DPD scintigraphy as a novel imaging modality for identification of skeletal muscle amyloid deposition in light-chain amyloidosis. *Amyloid*. 2016;23:134–5. <https://doi.org/10.3109/13506129.2016.1158160>.
- Puille M, Altland K, Linke RP, Steen-Muller MK, Kiett R, Steiner D, et al. 99mTc-DPD scintigraphy in transthyretin-related familial amyloidotic polyneuropathy. *Eur J Nucl Med Mol Imaging*. 2002;29:376–9.
- Quarta CC, Obici L, Guidalotti PL, Pieroni M, Longhi S, Perlini S, et al. High 99mTc-DPD myocardial uptake in a patient with apolipoprotein AI-related amyloidotic cardiomyopathy. *Amyloid*. 2013;20:48–51. <https://doi.org/10.3109/13506129.2012.746938>.
- Rao BK, Padmalatha C, Au Buchon J, Lieberman LM. Hepatic and splenic scintigraphy in idiopathic systemic amyloidosis. *Eur J Nucl Med*. 1981;6:143–6.
- Janssen S, Piers DA, van Rijswijk MH, Meijer S, Mandema E. Soft-tissue uptake of 99mTc-diphosphonate and 99mTc-pyrophosphate in amyloidosis. *Eur J Nucl Med*. 1990;16:663–70.
- Bokhari S, Castano A, Pozniakoff T, Deslisle S, Latif F, Maurer MS. (99m)Tc-pyrophosphate scintigraphy for differentiating light-chain cardiac amyloidosis from the transthyretin-related familial and senile cardiac amyloidoses. *Circ Cardiovasc Imaging*. 2013;6:195–201. <https://doi.org/10.1161/circimaging.112.000132>.
- Nakagawa M, Sekijima Y, Yazaki M, Tojo K, Yoshinaga T, Doden T, et al. Carpal tunnel syndrome: a common initial symptom of systemic wild-type ATTR (ATTRwt) amyloidosis. *Amyloid*. 2016;23:58–63. <https://doi.org/10.3109/13506129.2015.1135792>.
- Dorbala S, Vangala D, Semer J, Strader C, Bruyere JR Jr, Di Carli MF, et al. Imaging cardiac amyloidosis: a pilot study using ¹⁸F-florbetapir positron emission tomography. *Eur J Nucl Med Mol Imaging*. 2014;41:1652–62. <https://doi.org/10.1007/s00259-014-2787-6>.
- Osborne DR, Acuff SN, Stuckey A, Wall JS. A routine PET/CT protocol with streamlined calculations for assessing cardiac amyloidosis using (18)F-florbetapir. *Front Cardiovasc Med*. 2015;2:23. <https://doi.org/10.3389/fcvm.2015.00023>.
- Broski SM, Spinner RJ, Howe BM, Dispenzieri A, Johnson GB. ¹⁸F-Florbetapir and ¹⁸F-FDG PET/CT in systemic immunoglobulin light chain amyloidosis involving the peripheral nerves. *Clin Nucl Med*. 2016;41:e115–7. <https://doi.org/10.1097/rlu.0000000000000947>.
- García-González P, Sánchez-Jurado R, Cozar-Santiago MP, Ferrando-Beltrán M, Pérez-Rodríguez PL, Ferrer-Rebolledo J. Laryngeal and cardiac amyloidosis diagnosed by ¹⁸F-Florbetapir PET/CT. *Rev Esp Med Nucl Imagen Mol*. 2017;36:135–6. <https://doi.org/10.1016/j.remnm.2016.03.006>.
- Leung N, Ramirez-Alvarado M, Nasr SH, Kemp BJ, Johnson GB. Detection of ALECT2 amyloidosis by positron emission tomography-computed tomography imaging with florbetapir. *Br J Haematol*. 2017;177:12. <https://doi.org/10.1111/bjh.14519>.
- D'Estanque E, Chambert B, Moranne O, Kotzki PO, Boudousq V. ¹⁸F-Florbetaben: a new tool for amyloidosis staging? *Clin Nucl Med*. 2017;42:50–3. <https://doi.org/10.1097/rlu.0000000000001434>.
- Aprile C, Marinone G, Saponaro R, Bonino C, Merlini G. Cardiac and pleuropulmonary AL amyloid imaging with technetium-99m labelled aprotinin. *Eur J Nucl Med*. 1995;22:1393–401.
- Schaadt BK, Hendel HW, Gimsing P, Jonsson V, Pedersen H, Hesse B. 99mTc-aprotinin scintigraphy in amyloidosis. *J Nucl Med*. 2003;44:177–83.

29. Hawkins PN, Pepys MB. Imaging amyloidosis with radiolabelled SAP. *Eur J Nucl Med.* 1995;22:595–9.
30. Bokhari S, Shahzad R, Castano A, Maurer MS. Nuclear imaging modalities for cardiac amyloidosis. *J Nucl Cardiol.* 2014;21:175–84. <https://doi.org/10.1007/s12350-013-9803-2>.
31. Ohyama T, Shimokama T, Yoshikawa Y, Watanabe T. Splenic amyloidosis: correlations between chemical types of amyloid protein and morphological features. *Mod Pathol.* 1990;3:419–22.
32. Martins AC, Rosa AM, Costa E, Tavares C, Quadrado MJ, Murta JN. Ocular manifestations and therapeutic options in patients with familial amyloid polyneuropathy: a systematic review. *Biomed Res Int.* 2015;2015:282405. <https://doi.org/10.1155/2015/282405>.
33. Hachulla E, Janin A, Flipo RM, Saile R, Facon T, Bataille D, et al. Labial salivary gland biopsy is a reliable test for the diagnosis of primary and secondary amyloidosis. A prospective clinical and immunohistologic study in 59 patients. *Arthritis Rheum.* 1993;36:691–7.
34. de Paula EF, de Mello BL, de Carvalho DL, Della-Guardia B, de Almeida MD, Marins LV, et al. Minor salivary gland biopsy for the diagnosis of familial amyloid polyneuropathy. *Neurol Sci.* 2017;38:311–8. <https://doi.org/10.1007/s10072-016-2760-1>.
35. Villa F, Dionigi G, Tanda ML, Rovera F, Boni L. Amyloid goiter. *Int J Surg.* 2008;6(Suppl 1):S16–8. <https://doi.org/10.1016/j.ijisu.2008.12.025>.
36. Matsuda M, Gono T, Shimojima Y, Yoshida T, Katoh N, Hoshii Y, et al. AL amyloidosis manifesting as systemic lymphadenopathy. *Amyloid.* 2008;15:117–24. <https://doi.org/10.1080/13506120802006047>.
37. Kyle RA, Gertz MA. Primary systemic amyloidosis: clinical and laboratory features in 474 cases. *Semin Hematol.* 1995;32:45–59.
38. Matsuda M, Katoh N, Ikeda S. Clinical manifestations at diagnosis in Japanese patients with systemic AL amyloidosis: a retrospective study of 202 cases with a special attention to uncommon symptoms. *Intern Med.* 2014;53:403–12.